30th Annual International IEEE EMBS Conference
Vancouver, British Columbia, Canada, August 20-24, 2008

# Reliable Motion Artifact Detection for ECG Monitoring Systems with Dry Electrodes

Jörg Ottenbacher, Malte Kirst, Luciana Jatobá, Michal Huflejt, Ulrich Großmann, Wilhelm Stork

*Abstract*— **Reliable signals are the basic prerequisite for most mobile ECG monitoring applications. Especially when signals are analyzed automatically, capable motion artifact detection algorithms are of great importance. This article presents different artifact detection algorithms for ECG systems with dry electrodes. The algorithms are based on the measurement of additional parameters that are correlated with the artifacts. We describe a mobile measurement system and the procedure used for the evaluation of these algorithms. The algorithms are assessed based upon their effect on QRS detection. The best algorithm improved sensitivity (Se) from 98.7% to 99.8% and positive predictive value (+P) from 98.3% to 99.9%, while 15% of the signal was marked as artifact. This corresponds to a decrease in false positive and false negative detected beats by 89.9%. Different metrics to evaluate the performance of an artifact detection algorithm are presented.**

## I. INTRODUCTION

Ongoing progress in the area of wearable devices and smart clothing enable new applications of long-term mobile physiological monitoring. In such applications the amount of acquired data demands an automatic analysis or at least an automatic online pre-analysis. This is made difficult due to artifacts resulting from motions in daily life activities. To avoid failures caused by noisy signals and to be able to make reliable statements it is important to be able to estimate the signal quality.

Especially permanent ECG monitoring offers a wide range of promising applications, like wearable heart defibrillators, monitoring of risk patients or event recording. For permanent ECG monitoring applications the use of dry electrodes provides many advantages over standard adhesive electrodes [1] [2]. In this article we present different motion artifact detection algorithms for ECG systems with dry electrodes.

## II. MOTION ARTIFACTS

### A. Origin

Motion artifacts represent the most problematic source of noise in mobile ECG recordings. These artifacts are potentials that are superimposed onto the ECG signal. Motion artifacts from electrodes are produced by disturbing the electrode/electrolyte equilibrium potential. Artifacts from the skin are generated by the deformation of the skin under the electrode by changing the skin potential [3] [4] [2]. In contrast to other artifact sources, like interference from electrical fields, it is difficult to reduce motion artifacts by design. Motion artifacts can have amplitudes of several millivolts. They share the same frequency spectrum as ECG signals and the shape of motion artifacts can be very similar to ECG events. It is therefore very difficult to reliably detect artifacts only using the ECG signal.

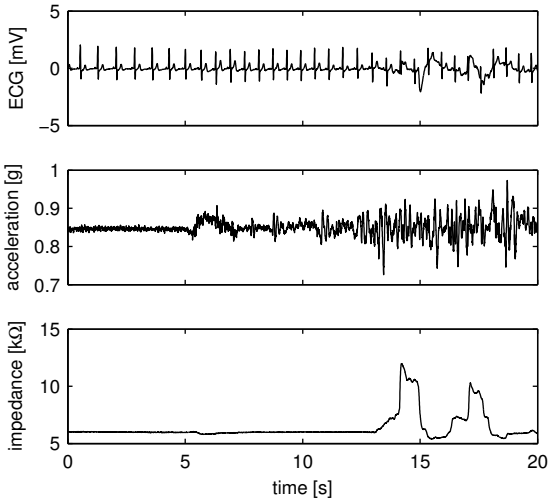


Fig. 1. Correlation of movement artifacts in different signals

### B. Correlated signals

A common approach to improve artifact detection is to use information from additional signals that correlate to the motion artifact [5] [6]. To use this method, a good correlation between the additional signal and the artifact and at best no correlation between the additional signal and the ECG signal is required. For a mobile ECG system, both electrode/skin impedance and electrode acceleration suggest itself as such an additional parameter. A low-power implementation of both parameters is possible. When using dry electrodes, electrode/skin impedance correlation is especially high. The change of skin stretch and pressure changes the contact area between electrode and skin and therefore the electrode skin conductivity [7]. Figure 1 shows a simultaneous recording of ECG, impedance and acceleration and correlation between the artifact in the ECG signal and impedance or acceleration.

J. Ottenbacher, L. Jatobá, U. Großmann and W. Stork are with the Institute for Information Processing Technology, University of Karlsruhe, 76131 Karlsruhe, Germany ottenbacher@itiv.uni-karlsruhe.de
jatoba@itiv.uni-karlsruhe.de
gross@itiv.uni-karlsruhe.de
stork@itiv.uni-karlsruhe.de

M. Kirst is with the FZI Research Center for Information Technology, 76131 Karlsruhe, Germany kirst@fzi.de

M. Huflejt is with the Department of Computer Science, University of Hamburg, Germany huflejt@informatik.uni-hamburg.de

978-1-4244-1815-2/08/$25.00 ©2008 IEEE. 

## III. INSTRUMENTATION AND MOBILE MEASSUREMENT SYSTEM

To be able to obtain realistic measurements, a mobile measurement system that allows the simultaneous acquisition of ECG signals, electrode acceleration and electrode/skin impedance was developed. A new analog front-end including A/D converters was integrated with a commercial Holter recoding system. The Holter recorder is used as a data logger and allows storing the measured raw data on compact flash cards over several hours.

The analog front-end allows the measurement of a one channel ECG with dry electrodes with a sample rate of 1 kHz. Two additional ECG channels for standard adhesive electrodes are also sampled with 1 kHz as a reference. The electrode impedance is measured separately at each of the dry electrodes and is sampled with 8 kHz. The sinusoidal current for impedance measurement has a frequency of 400 Hz and an amplitude $<1\,\mu$A. Each of the dry electrodes is equipped with a 3-axis acceleration sensor with a full-range of $\pm 6$ g. The dry electrodes are made of silver plates and are integrated into a chest belt with an elastic band and a velcro fastener. The electrode area is $2\,\text{cm}^2$. To be able to measure the impedance at each electrode individually, each electrode consists of two electrode plates.

We stored the complete raw data on flash cards. The further signal processing of the data is done in Matlab on a PC. The reconstruction of the impedance values is done with the help of dual lockin-amplifiers.

## IV. ARTIFACT DETECTION ALGORITHMS

The artifact detection algorithms we implemented consist of three steps: At first an artifact level, which expresses the intensity of artifacts in the ECG signal, is calculated. In a second step the generated artifact levels are post-processed and at last it is decided by means of a threshold if the ECG signal is marked as artifact region.

### A. Artifact level from impedance data

The impedance signals from each electrode are high pass filtered with a 4th order Butterworth with a cutoff frequency of 1 Hz.

An adaptive filter is used to estimate the artifact in the ECG signal from the impedance signals. Adaptive filters are always non-linear because the principle of superposition is not fulfilled [8]. Therefore the following different combinations of estimating artifacts were used:

- af{right + left}
- af{right − left}
- af{abs(right − left)}
- af{left} + af{right}
- af{left} − af{right}
- abs(af{right} − af{left})

Here af{x} means the application of an adaptive filter to the signal x. The LMS algorithm was used for the adaptive filter. The filter length was set to 100.

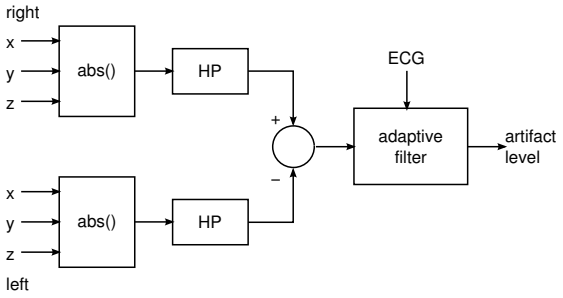


Fig. 2. Artifact level from acceleration data

### B. Artifact level from acceleration data

The calculation of artifact levels from acceleration data is very similar to the procedure with impedance data. At first the acceleration data was downsampled to 200 Hz. We used different ways to combine the three spacial dimensions of one acceleration sensor to a single value:

- geometric absolute value
- arithmetic mean
- scalar product of acceleration vector and first principal component of principal component analysis

The further processing was the same as with impedance data. Figure 2 shows an example of artifact level generation.

### C. Post-processing of artifact levels

The artifact levels were post-processed in three different ways

- no further processing
- artifact level is squared
- artifact level is squared and then filtered with a moving average filter with the length of 0.5 s

Finally we had 72 different artifact levels available for artifact detection.

### D. Thresholds and detection

If the artifact level exceeds a certain threshold the corresponding ECG signal region and 1s after it is marked as artifact. If the distance between two artifact regions is smaller than a defined minimum distance the two regions are combined. Fig. 3 shows an example of two marked artifacts.

## V. MEASUREMENTS

With the mobile measurement system we made recordings on 14 subjects (fig. 4). The persons had to undergo a

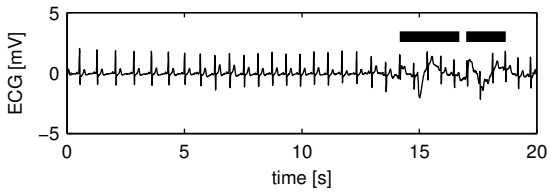


Fig. 3. ECG with two detected artifact regions (horizontal bars)

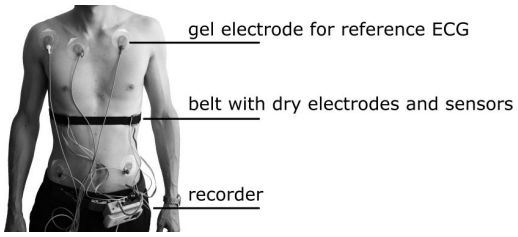


Fig. 4. Measurement setup for ECG, impedance and acceleration measuring

defined procedure with different daily life activities including activities that often provoke artifacts in ECG recordings, like climbing stairs and jogging. The total duration of each recording was about one hour. The dry electrode chest belt was worn in the height of the sternum. The subjects were instructed to wear the chest belt only as tight as they could imagine to wear it over a very long period of time. Additionally we recorded the Einthoven I and II leads with standard adhesive electrodes. From two measurements we discarded regions in which the electrode belt came loose completely. For further evaluation we had about 14 hours of utilizable data.

## VI. EVALUATION AND RESULTS

The quality of the artifact detection methods were evaluated by comparing the detection quality of different QRS detectors with and without artifact detection. At first a QRS reference trigger list was created manually by the help of a professional Holter analysis software for each recording.

### A. Comparison of QRS detectors

We compared three QRS detectors in respect of detection performance on signals contaminated with motion artifacts:

- OSEA: QRS detector from the Open Source ECG Analysis software [9]
- PADSY: QRS detector that is part of the patient diagnostic system PADSY [10]
- MOBD: own implementation of the Multiplication of Backward Difference QRS detector [11]

With a sensitivity of 98.73% and a positive predictive value of 98.25% the OSEA QRS detector performed best and is also well-balanced in sensitivity and positive predictive value. OSEA was used for all further studies.

### B. Effect of artifact detection algorithms on QRS detection

To be able to compare the performance of the proposed artifact detection algorithms, the threshold for each algorithm was set that 15% of the recorded data was marked as artifact.

Now, the number of TP, FP and FN beats inside and outside the marked artifact regions were determined and the new values for sensitivity $Se_{qrs}$ and positive predictive value $+P_{qrs}$ for OSEA were calculated. The results for the 15%-threshold are shown in Figure 5.

A clear separation of algorithms based on acceleration and impedance can be seen. One algorithm based on impedance (adaptive filter: af$\{$right $-$ left$\}$, post-processing: squaring and moving average) improved the sensitivity to $Se_{qrs} =$ 99.8% and the positive predictive value to $+P_{qrs} = 99.9\%$. This is equivalent to a decrease in false positive and false negative QRS beats of 89.9%.

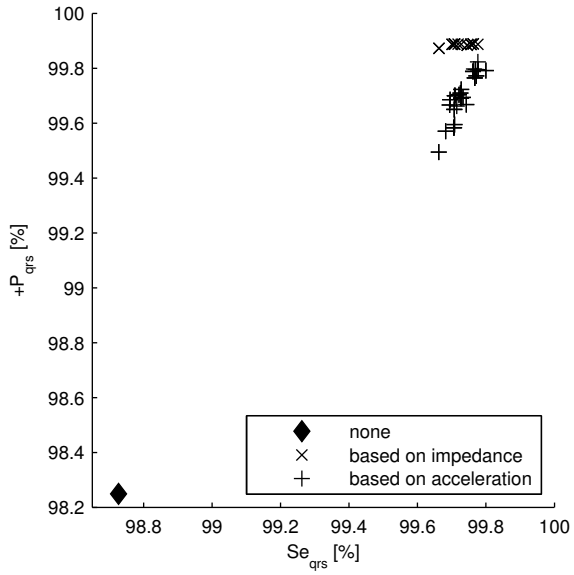


Fig. 5. Effect of artifact detection on sensitivity and positive predictive value of QRS detection

### C. Performance comparison of artifact detection algorithms

Considering only $Se_{qrs}$ and $+P_{qrs}$ does not take the information loss of TP beats inside regions marked as artifact into account. To improve this situation, additional metrics are needed. If it is assumed that the QRS detector has an accuracy of 100% if no artifacts are available in the ECG signal, it is possible to determine artifact regions by using QRS beat detection data.

This means that false positive and false negative QRS beats inside a region marked as artifact are corresponding to true positive detected artifacts $TP_{ad} = FN_i + FP_i$. True positive QRS beats inside a region marked as artifact correspond to false positive detected artifacts $FP_{ad} = TP_i$, while true positive QRS beats outside correspond to true negative artifact detections $TN_{ad} = TP_o$. False negative artifact detection can be written as the sum of false positive and false negative QRS beats outside regions marked as artifact $FN_{ad} = FN_o + FP_o$. The sensitivity and specificity of the artifact detector is then

$$Se_{ad} = \frac{TP_{ad}}{TP_{ad} + FN_{ad}} = \frac{FN_i + FP_i}{FN_i + FP_i + FN_o + FP_o} \quad (1)$$

$$Sp_{ad} = \frac{TN_{ad}}{TN_{ad} + FP_{ad}} = \frac{TP_o}{TP_o + TP_i} \quad (2)$$

These metrics can now be used to compare the performance and characteristics of the artifact detection algorithms.

For each artifact detection algorithm we calculated threshold values so that respectively 2%, 5%, 10%, 15%, 20%, 25% and 55% of the recorded data was marked as artifact. For every artifact detection algorithm and threshold we calculated the sensitivity $Se_{ad}$ and specificity $Sp_{ad}$. With

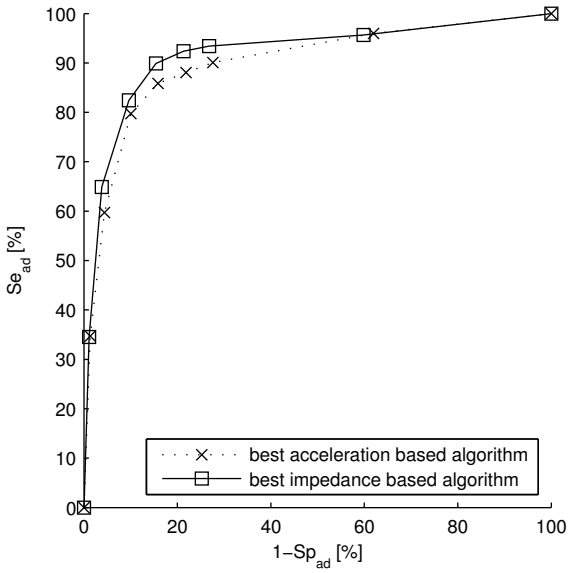


Fig. 6. ROC graph for the best impedance and acceleration based artifact detection algorithm

this data the performance can be visualized in a receiver operating characteristics (ROC) graph. From ROC graphs the artifact detection algorithm with the best detection performance can be identified by comparing the area under the ROC curve (AUC). Figure 6 shows the ROC graph for the best impedance and acceleration based artifact detection algorithm, table I the corresponding AUC values.

To find the threshold where a specific artifact detection algorithm has its highest detection accuracy, that point of the ROC curve has to be identified, where its gradient is one. However, the graphs can also help to identify an artifact detection algorithm that performs best for a specific application. E. g. for risk monitoring applications, loss of information should be minimized and one would accept more false alarms. So an algorithm with best performance at a higher specificity level can be chosen.

TABLE I
AUC VALUES FOR THE BEST ARTIFACT DETECTION ALGORITHMS

| algorithm | AUC |
|---|---|
| best acceleration based algorithm | 0.8999 |
| best impedance based algorithm | 0.9179 |

## VII. DISCUSSION AND OUTLOOK

All presented artifact detection algorithms have a positive effect on QRS detection performance. In conjunction with the OSEA QRS detector the algorithms based on impedance perform slightly better than the ones based on acceleration data. A decrease in false positive and false negative QRS beat detections of 89.9% was achieved. The instrumentation needed for impedance and acceleration measurement can be implemented in a mobile ECG monitoring system with moderate cost.

For the evaluation of these artifact detection algorithms a criteria is needed, which has been extracted from the QRS detection results. The assumption is that a QRS detector only has false detections when artifacts are present. For this reason the dependence between artifact detection algorithm and QRS detection algorithm is considerable. I. e. artifact detectors selected with the help of one QRS detector do not necessarily have to perform best in conjunction with another QRS detector. This also means that a selected artifact detection algorithm may not be sufficient for other or further ECG analysis methods like heart rate variability HRV or calculation of pulse transit time (PTT).

Metrics like sensitivity $Se_{ad}$ and specificity $Sp_{ad}$ and the visualization of the artifact detection performance in ROC graphs can help identifying the best algorithm for a specific application.

Probably the presented artifact detection algorithms can be further improved by optimizing various parameters like adaptive filtering parameters, timeouts or by combining acceleration and impedance information. A further improvement of QRS detection is surely possible if QRS detector and artifact detector are better integrated (e. g. influence adapting of inner thresholds of the QRS detector).

## VIII. ACKNOWLEDGMENTS

This work has been kindly supported by the German government BMBF projects CALM and MµGUARD and by Medset Medizintechnik GmbH. The authors thank the Universitätsklinik Erlangen for supporting the measurements.

## REFERENCES

[1] A. Searle and L. Kirkup, "A direct comparison of wet, dry and insulating bioelectric recording electrodes," *Physiol Meas*, vol. 21, no. 2, pp. 271–83, May 2000.

[2] J. Ottenbacher, L. Jatobá, U. Großmann, W. Stork, and K. Müller-Glaser, "Ecg electrodes for a context-aware cardiac permanent monitoring system," in *World Congress on Medical Physics and Biomedical Engineering 2006*, ser. IFMBE Proceedings, vol. 14. Springer Berlin Heidelberg, Juli 2006.

[3] H. de Talhouet and J. Webster, "The origin of skin-stretch-caused motion artifacts under electrodes." *Physiological Measurement*, vol. 17, no. 2, pp. 81–93, May 1996.

[4] W. K. Vos, P. Bergveld, and E. Marani, "Low frequency changes in skin surface potentials by skin compression: experimental results and theories." *Arch Physiol Biochem*, vol. 111, no. 4, pp. 369–376, Oct 2003. [Online]. Available: http://dx.doi.org/10.1080/13813450312331337621

[5] P. Hamilton, M. G. Curley, R. Aimi, and C. Sae-Hau, "Comparison of methods for adaptive removal of motion artifact," *Computers in Cardiology*, pp. 383 – 386, 2000.

[6] D. Tong, K. Bartels, and K. Honeyager, "Adaptive reduction of motion artifact in the electrocardiogram," *EMBS/BMES Conference, Proceedings of the Second Joint*, vol. 2, pp. 1403– 1404, 2002.

[7] J. Ottenbacher, M. Kirst, L. Jatobá, U. Großmann, and W. Stork, "An approach to reliable motion artifact detection for mobile long-term ecg monitoring systems using dry electrodes," in *IV Latin American Congress on Biomedical Engineering 2007*, ser. IFMBE Proceedings, vol. 18. Springer Berlin Heidelberg, November 2007, pp. 440–443.

[8] S. Haykin, *Adaptive Filter Theory*. Prentice Hall, 2001.

[9] P. S. Hamilton, *Open Source ECG Analysis Software Documentation*, E.P. Limited, 2002, http://www.eplimited.com.

[10] M. Medizintechnik, "Padsy – patient diagnostic system," 2008. [Online]. Available: http://www.medset.com/

[11] Y. Sun, S. Suppappola, and T. A. Wrublewski, "Microcontroller-based real-time qrs detection." *Biomed Instrum Technol*, vol. 26, no. 6, pp. 477–484, 1992.